

## Supplementary Methods

**MLN4924 Synthesis.** *General Synthetic Procedures.* All solvents and chemicals were purchased from Sigma-Aldrich, Acros, Fisher, or Chembridge and were used as received without further purification. Purity and characterization of compounds were established by a combination of liquid chromatography-mass spectroscopy (LC-MS) and NMR analytical techniques. Silica gel column chromatography was carried out using prepacked silica cartridges from RediSep (ISCO Ltd.) and eluted using an Isco Companion system. <sup>1</sup>H NMR spectra were acquired on Jeol or Bruker 400 MHz spectrometers. Chemical shifts are reported in ppm from residual solvent peaks. Reversed-phase HPLC-MS analyses were performed on a Shimadzu 2010EV LCMS using the following conditions: Kromisil C18 column (reverse phase, 4.6 mm × 50 mm); a linear gradient from 10% acetonitrile and 90% water to 95% acetonitrile and 5% water over 4.5 min; flow rate of 1 mL/min; UV photo-diode array detection from 200 to 300 nm.

*(3R,3aS,6aS)-3-hydroxy-3,3a,4,6a-tetrahydro-2H-cyclopenta[b]furan-2-one.* A solution of aqueous glyoxylic acid (50% w/v, 50 mmol), water (10 ml), and freshly distilled cyclopentadiene (65 mmol) were combined at 0°C and stirred vigorously. After slowly warming to ambient temperature, the reaction was stirred for an additional 5 days. The solution was extracted with heptane to remove the excess cyclopentadiene and then with ethyl acetate. The organic layers were collected, washed with sodium bicarbonate and brine, and the solvent was removed via rotary evaporation to provide a yellow oil. Chromatography over silica with hexane:ethyl acetate (2:3) provided two sets of fractions. The first fractions contained (3S,3aS,6aS)-3-hydroxy-3,3a,4,6a-tetrahydro-2H-cyclopenta[b]furan-2-one. The later eluting fractions contained the product, (3R,3aS,6aS)-3-hydroxy-3,3a,4,6a-tetrahydro-2H-cyclopenta[b]furan-2-one, as a tan solid after evaporation (32%). <sup>1</sup>H NMR (400 MHz, CDCl<sub>3</sub>): δ 6.26 (m, 1H), 5.94 (m, 1H), 5.34 (m, 1H), 4.71 (d, *J* = 24 Hz, 1H), 3.31 (s, 1H), 3.22 (m, 1H), 2.75 (m, 1H), 2.46 (m, 1H).

*(1S,5S)-5-(hydroxymethyl)cyclopent-2-enol*. To a solution of *(3R,3aS,6aS)-3-hydroxy-3,3a,4,6a-tetrahydro-2H-cyclopenta[b]furan-2-one* (15 mmol) in anhydrous tetrahydrofuran (10 ml) was added lithium aluminum hydride (20 mmol) and the mixture was heated to reflux and stirred for 1 h. The mixture was cooled and aqueous sodium sulfate solution was added followed by stirring at RT for 1 h. The mixture was filtered and extracted with ethyl acetate. After evaporation, the crude triol was taken up in a 1:1 mixture of methyl *tert*-butyl ether and brine and cooled to 0°C. Sodium periodate (12.5 mmol) was added and the mixture was stirred for 2h. After filtration and evaporation, the crude residue was dissolved in ethanol and treated with sodium borohydride (15 mmol) and stirred overnight. The mixture was diluted with brine and extracted with ethyl acetate. The solvent was removed and the residue was purified by flash chromatography to yield the product as a colorless liquid (47%). <sup>1</sup>H NMR (400 MHz, CDCl<sub>3</sub>): δ 5.95 (m, 1H), 5.80 (m, 1H), 4.88 (d, *J* = 18 Hz, 1H), 3.77 (m, 2H), 2.50 (m, 1H), 2.32 (m, 2H).

*(4aS,7aS)-2-(4-methoxyphenyl)-4,4a,5,7a-tetrahydrocyclopenta[d][1,3]dioxine*. To a solution of *(1S,5S)-5-(hydroxymethyl)cyclopent-2-enol* (7.0 mmol) in toluene (25 ml) at RT was added anisaldehyde (10 mmol) and *p*-toluenesulfonic acid (a catalytic amount). The mixture was heated for 3 h at reflux under nitrogen with a Dean–Stark trap to remove water. The mixture was cooled, washed with 10% NaHCO<sub>3</sub>, then with brine. Following concentration, the crude product was purified on a silica column (hexane:ethyl acetate gradient, 4:1–2:1) to afford the title compound (89%). <sup>1</sup>H NMR (400 MHz, CDCl<sub>3</sub>): δ 7.40 (d, *J* = 22 Hz, 2H), 6.87 (d, *J* = 22 Hz, 2H), 5.91 (m, 1H), 5.87 (m, 1H), 5.67 (s, 1H), 3.77 (s, 3H), 3.65 (m, 3H), 2.41 (m, 2H), 2.20 (m, 1H).

*(4aS,6R,7S,7aR)-6-(4-(((S)-2,3-dihydro-1H-inden-1-yl)amino)-7H-pyrrolo[2,3-d]pyrimidin-7-yl)-2-(4-methoxyphenyl)hexahydrocyclopenta[d][1,3]dioxin-7-ol*. To a solution of *(4aS,7aS)-2-(4-methoxyphenyl)-4,4a,5,7a-tetrahydrocyclopenta[d][1,3]dioxine* (5.0 mmol) in dichloromethane (20 ml) was added *m*-chloroperoxybenzoic acid (7.5 mmol) and the mixture was stirred at RT overnight. The

solvent was removed and the residue partitioned between diethyl ether and water. The organic layer was separated and the solvent was removed to obtain the crude epoxide which was dissolved in DMF (3 ml) and added to a pre-mixed solution of *N*-[(1*S*)-2,3-dihydro-1*H*-inden-1-yl]-7*H*-pyrrolo[2,3-*d*]pyrimidin-4-amine (4.0 mmol) and sodium hydride (4.0 mmol) in DMF (7 ml). The reaction was stirred at 100°C for 3 h, quenched with brine, and extracted with ethyl acetate. The organic layer was separated and concentrated and the residue was purified by flash chromatography using an ethyl acetate:hexanes gradient to furnish the title compound (42%). ESI-MS: *m/z* 499 [M + H]<sup>+</sup> (TFA); RP-HPLC: R<sub>t</sub> = 2.7 min.

*((1S,2S,4R)-4-(4-(((S)-2,3-dihydro-1H-inden-1-yl)amino)-7H-pyrrolo[2,3-d]pyrimidin-7-yl)-2-hydroxycyclopentyl)methyl sulfamate, hydrochloride salt (MLN4924)*. (4*aS*,6*R*,7*S*,7*aR*)-6-(4-(((*S*)-2,3-dihydro-1*H*-inden-1-yl)amino)-7*H*-pyrrolo[2,3-*d*]pyrimidin-7-yl)-2-(4-methoxyphenyl)hexahydrocyclopenta[*d*][1,3]dioxin-7-ol (2.0 mmol), 1,1'-thiocarbonyl diimidazole (5.0 mmol), and DMAP (0.54 mmol) in THF (6.00 ml) were stirred for 24 h at 80°C. After the mixture was concentrated, the residue was purified by silica gel chromatography (hexan:ethyl acetate, 4:1) to afford the thiocarbonylimidazoyloxy intermediate. This intermediate was suspended in toluene (5 ml) and treated with tri-*n*-butyltin hydride (10 mmol) and 2,2'-azo-bis-isobutyronitrile (0.5 mmol) followed by heating at reflux for 1 h. The solvent was removed and the product was passed through a silica plug to separate the excess tin byproducts. The crude recovered product was stirred in a 1:1:1 mixture of acetic acid:tetrahydrofuran:water (6 ml) for 48 h, concentrated and purified by reversed-phase chromatography. This product (0.5 mmol) was subsequently dissolved in tetrahydrofuran (10 ml) and treated with Hunig's base (1.0 mmol) and [(Diphenylamino)carbonyl] sulfamoyl chloride (0.7 mmol) followed by stirring at RT for 1 h. The mixture was diluted with 1M hydrochloric acid solution and extracted with ethyl acetate. The product was isolated by reversed-phase HPLC (water:acetonitrile, 10-95%), and the concentrated fractions were treated with a minimal amount of 2M hydrochloric acid in dioxane, frozen and lyophilized to afford the title compound (13%). <sup>1</sup>H NMR (400 MHz, CH<sub>3</sub>OD): δ

8.314 (s, 1H), 7.55 (s, 1H), 7.37 (m, 3H), 7.29 (m, 1H), 6.97 (s, 1H), 5.56 (m, 2H), 4.56 (m, 1H), 4.41 (m, 1H), 4.23 (m, 1H), 3.16 (m, 1H), 3.05 (m, 1H), 2.90 (m, 1H), 2.76 (m, 1H), 2.36 (m, 3H), 2.16 (m, 2H). ESI-MS:  $m/z$  444  $[M + H]^+$  (TFA); RP-HPLC:  $R_t = 1.3$  min.

**Isolation of HCT116 cells resistant to MLN4924.** HCT116 cells (ATCC) were cultured in McCoy's 5A (Invitrogen) with 10% FBS. Cells were plated at  $2 \times 10^5$  per well in a 6 well plate and after 24 hours, DMSO (0.1% final) or increasing concentrations of MLN4924 (.001, .003, .01, .03, .1, .3, 1, 3  $\mu$ M) were added, with the culture media changed in the presence of the molecule every 48 hours. At MLN4924 concentrations below 0.1  $\mu$ M, the cells appeared unaffected and were discarded while those cultured with MLN4924 concentrations  $\geq 1$   $\mu$ M had 99%+ cell death as judged by trypan blue staining after 5 days of treatment. After 9 days, cell growth was observed in 1  $\mu$ M treated cultures and after 17 days these cells were transferred to a 10  $\text{cm}^2$  plate with the MLN4924 concentration increased to 1.5  $\mu$ M. The MLN4924 concentration was increased to 2  $\mu$ M at Day 21 and 3  $\mu$ M at Day 25. These HMR (HCT116 MLN4924 resistant) cells were maintained in 3  $\mu$ M MLN4924 unless where noted.

**Cell Proliferation and Viability Assays.** For cell proliferation measurements, HMR and HMS cells were plated at  $10^5$  cells per well in a 6-well plate and after 24 hours, DMSO (0.1% final concentration) or 3  $\mu$ M MLN4924 was added. After 24, 48, and 72 hours, cells were trypsinized and counted using a TC10 Automated Cell Counter (Bio-Rad). Live cell counts were obtained using trypan blue exclusion. Culture media were replenished during the experiment every 24 hours. Cell numbers represent triplicate measurements with error bars representing the standard error. The resulting data were analyzed in GraphPad Prism and fit to an exponential growth equation ( $Y = Y_0 e^{kt}$ ) where  $Y_0$  is the number of cells at the start of the experiment,  $k$  is a rate constant, and  $t$  is time. From this formula,  $k$

values of  $0.0370 \pm 0.0001$  hours<sup>-1</sup> for HMS,  $0.0346 \pm 0.0017$  hours<sup>-1</sup> for HMR, and  $0.0306 \pm 0.0021$  hours<sup>-1</sup> for HMR + MLN4924 were obtained with doubling times of 18.76 hours (95% confidence interval, CI: 17.75-19.89), 20.04 hours (CI: 18.04-22.54), and 22.64 hours (CI: 19.64-26.73), respectively. Data obtained for HMS cells treated with MLN4924 could not be fitted to this equation due to MLN4924-induced cell death.

For cell viability measurements, cells were plated at 4000 cells per well in a 96 well plate. After 24 hours, media were added containing 3-fold serial dilutions of MLN4924 from a maximum of 20  $\mu$ M or bortezomib from 2  $\mu$ M. Following a 48 hour treatment, cellular ATP content was measured using Cell Titer-Glo Luminescent Viability Assay (Promega) with plates read on a Turner Veritas Luminometer. These measurements were normalized for each treatment or cell line internally for each replicate with the maximum response (i.e., the lowest measurement) subtracted from all measurements and DMSO or the highest measured value set as 100%. The resulting values were averaged and analyzed in GraphPad Prism using non-linear regression analyses of log(inhibitor) vs. % viability using a four-parameter dose response curve and constraining the bottom of curves to 0. Data points are the mean (n=3) with error bars representing standard error.

**Gene Expression Profiling.** Total RNA was prepared from  $2 \times 10^6$  HMR (grown in the presence of 3  $\mu$ M MLN4924) or HMS (DMSO or treated with 3  $\mu$ M MLN4924 for 8 and 24 hours) using an RNeasy Mini Kit (Qiagen) and performed in triplicate. Labeled cRNA samples were generated and hybridized to an Illumina HumanHT-12 v4 Expression BeadChip prior to analysis on an Illumina BeadStation 500. Data analysis was performed by the Sanford-Burnham Medical Research Institute (SBMRI) Informatics and Data Management Shared Resources. Raw data were processed in Genome Studio (Illumina) and further analyzed in Genomics Suite (Partek). Downstream analyses included log<sub>2</sub> transformation of gene intensity data (with offset 1) followed by quantile normalization and determination of differentially

expressed genes. Differentially expressed genes between cell lines and conditions and fold change values were determined using ANOVA as implemented in Genomics Suite.

Data sets were initially filtered for genes involved in the gene ontology term "the process of the addition or removal of electrons". No statistically significant differences in the expression of the resulting 93 genes were identified. Hierarchical clustering of a subset of genes was performed on standardized data (shift to mean of zero and scaling to standard deviation of one for every sample). Average linkage clustering was performed using Euclidian distance. Supplementary Fig. 2 represents a heat map of standardized expression of 69 cytochrome P450 family members as expression of these are often altered in response to small molecules.

**MLN4924 Uptake and Retention.** HMS and HMR cells were plated at  $5 \times 10^6$  cells per  $10 \text{ cm}^2$  plate and after 24 hours, DMSO (0 time point) or  $3 \text{ }\mu\text{M}$  MLN4924 was added. Samples were prepared after 5, 30, 60, and 180 minutes post-MLN4924 addition. At each time point, cells were washed 3 times with cold PBS and scraped into 1 ml Quenching Solution (water:acetonitrile (20:80) with 0.05% formic acid). The samples were centrifuged and the supernatant was mixed 1:1 with Quenching Solution containing an internal standard ( $2.5 \text{ }\mu\text{M}$  indomethacin). After centrifugation, the supernatant was transferred to an autosampler vial and relative concentrations were assessed by LC-MS/MS in multiple reaction monitoring (MRM) mode. LC-MS/MS was performed using a Prominence liquid chromatography system (Shimadzu) directly coupled to an API3000 triple quadrupole mass spectrometry (Applied Biosystems) using MRM. Chromatography was carried out using gradient elution (water-acetonitrile) on a C18 reversed-phase column (Kromasil 100  $5 \text{ }\mu\text{M}$  C18 50 mm x 2.1 mm ID, Peeke Scientific) at a flow rate of 0.4 ml/min. The ratio of the peak area of MLN4924 to the peak area of the internal standard was determined using Analyst 1.4.2 software (Applied Biosystems). Data are expressed as the average ( $n=3$ ) ratio of measured peak areas for MLN4924 and indomethacin with SEM error bars.

**Protein Expression Analyses.** The following antibodies were used: NEDD8 (Invitrogen, 34-1400), NRF2 (Santa Cruz, sc-722), p27 (BD Biosciences, 610241), CDT1 (Millipore, 06-1295), Cyclin E (Invitrogen, AHF0162), p21 (BioSource, AHZ0392), PARP 214/215 cleavage site specific antibody (Invitrogen, 44698G), GAPDH (Millipore, MAB374),  $\alpha$ -tubulin (Invitrogen, 32-2500), UBA3 (Sigma, HPA034873), APPBP1/ NAE1 (Abnova, H00008883-A01), and Ubiquitin (Santa Cruz, sc-8017)

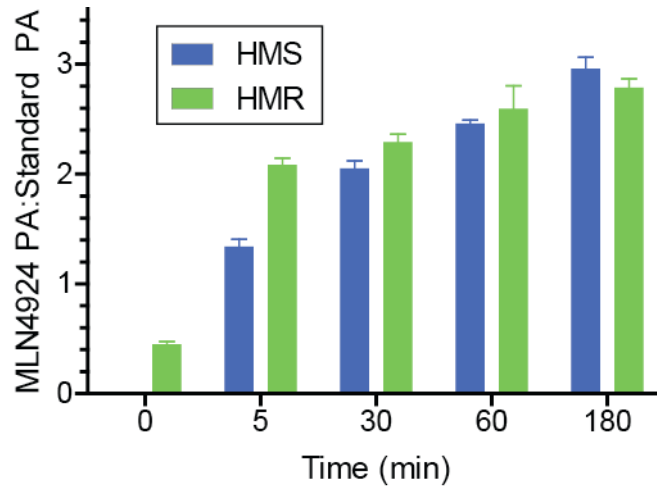
**Recombinant NAE and NEDD8.** The human open reading frames for ULA1, UBA3 (isoform 1), and NEDD8 were PCR amplified from the MegaMan Human Transcriptome Library (Agilent) and NAE1 and UBA3 were cloned into pFastBac1 (Invitrogen) and NEDD8 cloned into pET11b (Novagen). UBA3 included C-terminal sequences to encode a hexahistidine tag for NAE purification. UBA3 A171T was generated by QuikChange (Agilent). Baculoviruses were prepared using the FastBac system (Invitrogen). After 48 hours of co-infecting Hi5 cultures ( $10^6$  cells/ml, 100 ml) with NAE1 and UBA3 or UBA3 A171T baculoviruses, NAE complexes were purified by Ni-NTA chromatography and desalted into 25 mM HEPES pH7.6, 100 mM NaCl, and 10% glycerol. NEDD8 was expressed in Rosetta 2 *E.coli* (Novagen), purified by SP Sepharose chromatography using 50 mM ammonium acetate pH 4.5, a linear gradient of 100 to 500 mM NaCl, 1 mM EDTA, and 1 mM DTT, and desalted as described for NAE complexes. Protein concentrations were measured from Coomassie stained gels scanned on a Licor Odyssey, using known amounts of purified BSA to generate a standard curve and the instrument's analysis software. See Supplementary Fig. 7.

**ATP:PPi Exchange Assay.** The assay is based on a published method (Brownell et al., 2010; Bruzzese et al., 2009). Experiments were performed such that NAE or NAE (UBA3 A171T) was

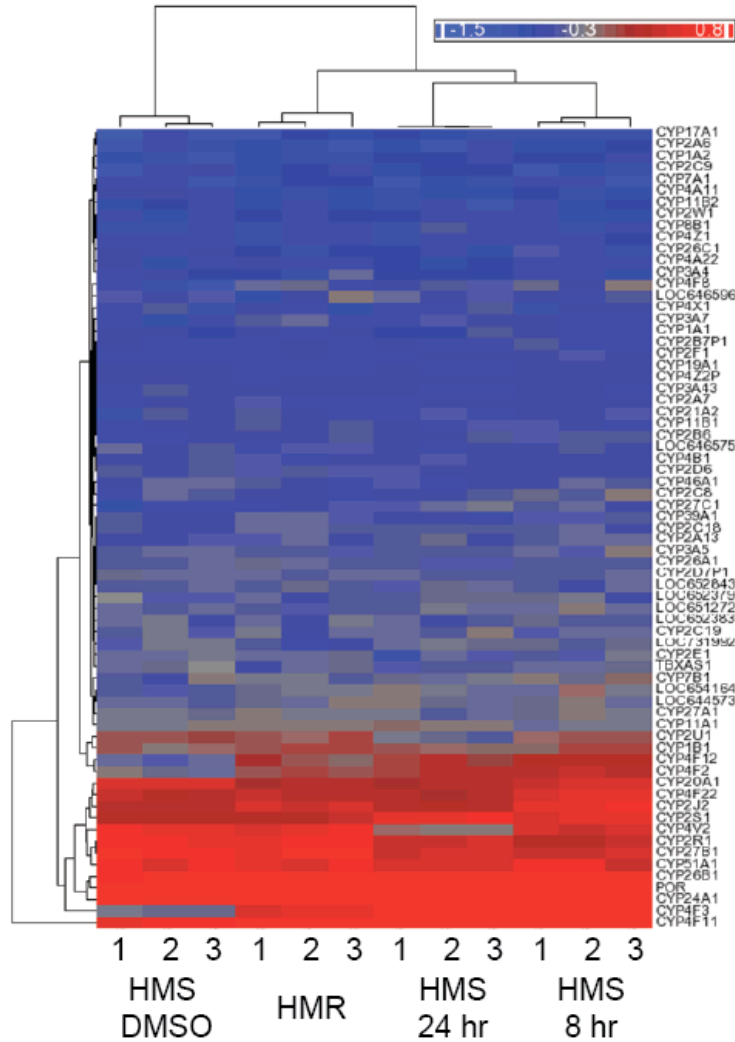
dispensed into a 96-well plate and pre-mixed with titrants (MLN4924, ATP, or PPI) and other assay components, including 50 cpm/pmol [<sup>32</sup>P] PPI. Reactions (50 μl final volume) were initiated by the addition of NEDD8 to 1 μM and incubated at 37°C for 30 minutes prior to termination with 400 μl Stop solution (5% TCA, 10 mM PPI). Quenched reactions were transferred to activated charcoal paper using vacuum driven transfer through a Minifold I dot blot system (Whatman). Wells were washed four times with 250 μl Wash Solution (2% TCA, 10 mM PPI) after which the filter was removed from the manifold and washed 5 times with 100 ml Wash Solution over 25 minutes. The processed filter was air dried and exposed to a phosphor screen prior to imaging on a Fuji FLA-5100. Resulting signals representing NAE generated radiolabeled ATP from phosphor screen scans were quantified using Multi Gauge software and ATP standards.

The assay buffer used was 25 mM HEPES pH 7.6, 5 mM MgCl<sub>2</sub>, 25 mM NaCl, 0.5 mM DTT. All experiments used NAE and NAE (UBA3 A171T) at 10 nM and NEDD8 at 1 μM final concentrations. MLN4924 titrations used 11 2-fold serial dilutions from 10 μM final concentration and a DMSO only control, 100 μM PPI with 50 cpm/pmol [<sup>32</sup>P] PPI and either 100 μM (Fig 4A) or 1 mM (Fig. 4B) ATP. ATP titrations (Fig. 4C) used 11 2-fold serial dilutions from 2 mM final concentration and a no ATP control with 1 mM PPI containing 50 cpm/pmol [<sup>32</sup>P] PPI. PPI titrations (Fig. 4D) used 11 2-fold serial dilutions from 1 mM final concentration and a no PPI control with 2 mM ATP. All reactions were performed in triplicate and measurements are expressed as the mean with error bars representing the SEM. Raw data are shown in Supplementary Fig. 8. Data analyses used GraphPad Prism software and a nonlinear regression algorithm to measure  $k_{cat}$  and extract other best-fit values from plots of rates of ATP synthesis vs. substrate concentration.

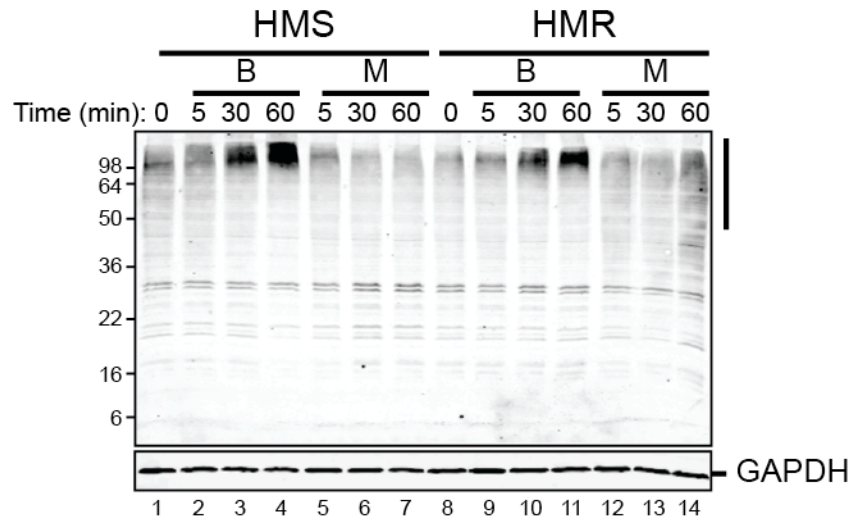




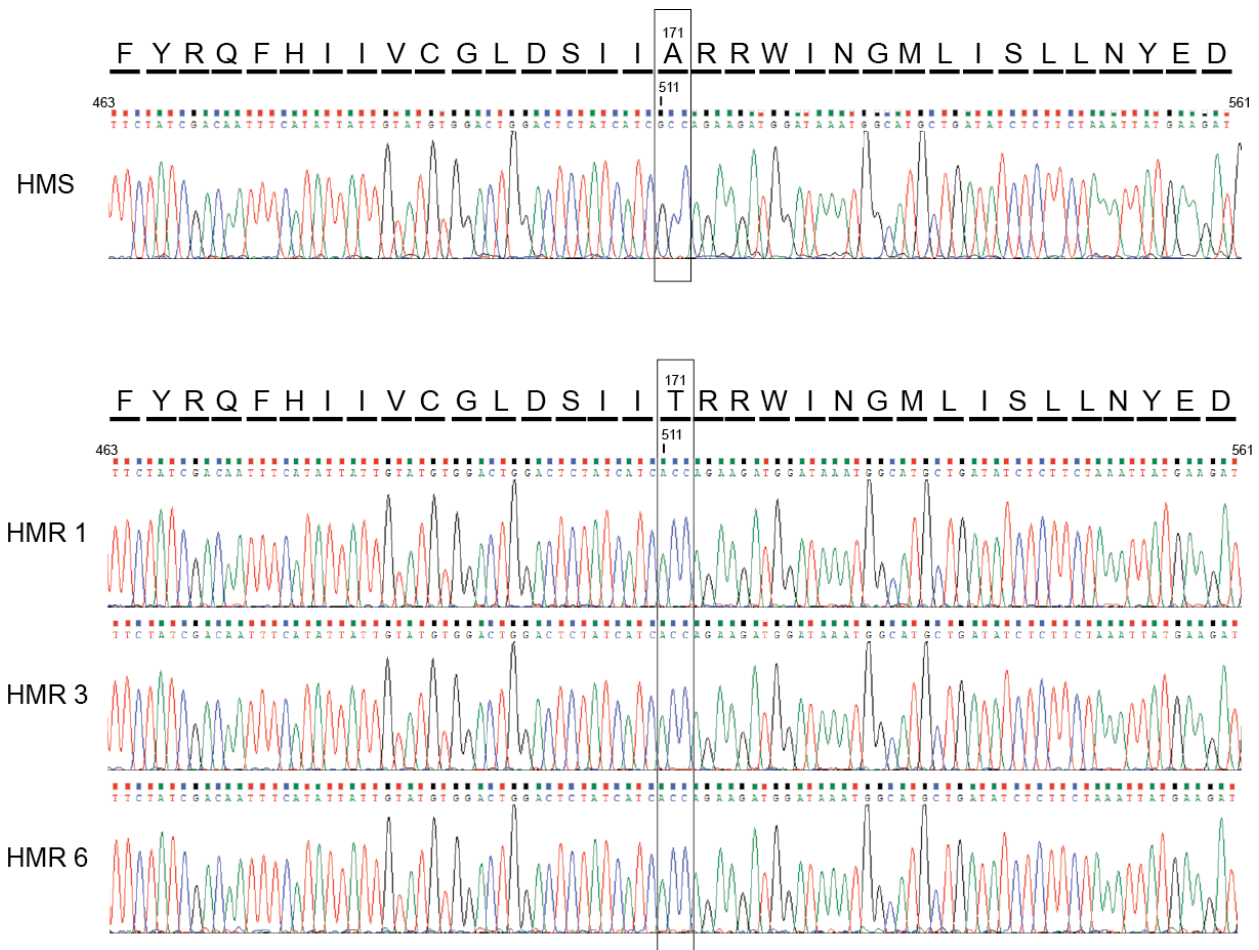
**Supplementary Figure 1 MLN4924 uptake and retention in HMS and HMR cells.** We measured the intracellular levels of MLN4924 using liquid chromatography tandem mass spectrometry (LC-MS/MS). Extracts from HMS and HMR cells were analyzed at various times after addition of 3  $\mu$ M MLN4924 using indomethacin as an internal standard. The peak area (PA) of MLN4924 and indomethacin were quantified and expressed as a ratio of MLN4924 PA:Standard PA. Data points represent the mean (n=3) with SEM error bars. HMR cells, cultured in the presence of MLN4924, had low levels of MLN4924 at the start of the experiment and higher levels of MLN4924 than HMS cells after 5 minutes, reflecting the maintenance of these cells in media containing MLN4924. However, HMS and HMR cells had similar amounts of MLN4924 after 30 minutes and were essentially indistinguishable over the rest of the 180 minute experiment. From these experiments, no obvious differences in the uptake or retention of MLN4924 were observed between HMS and HMR cells.



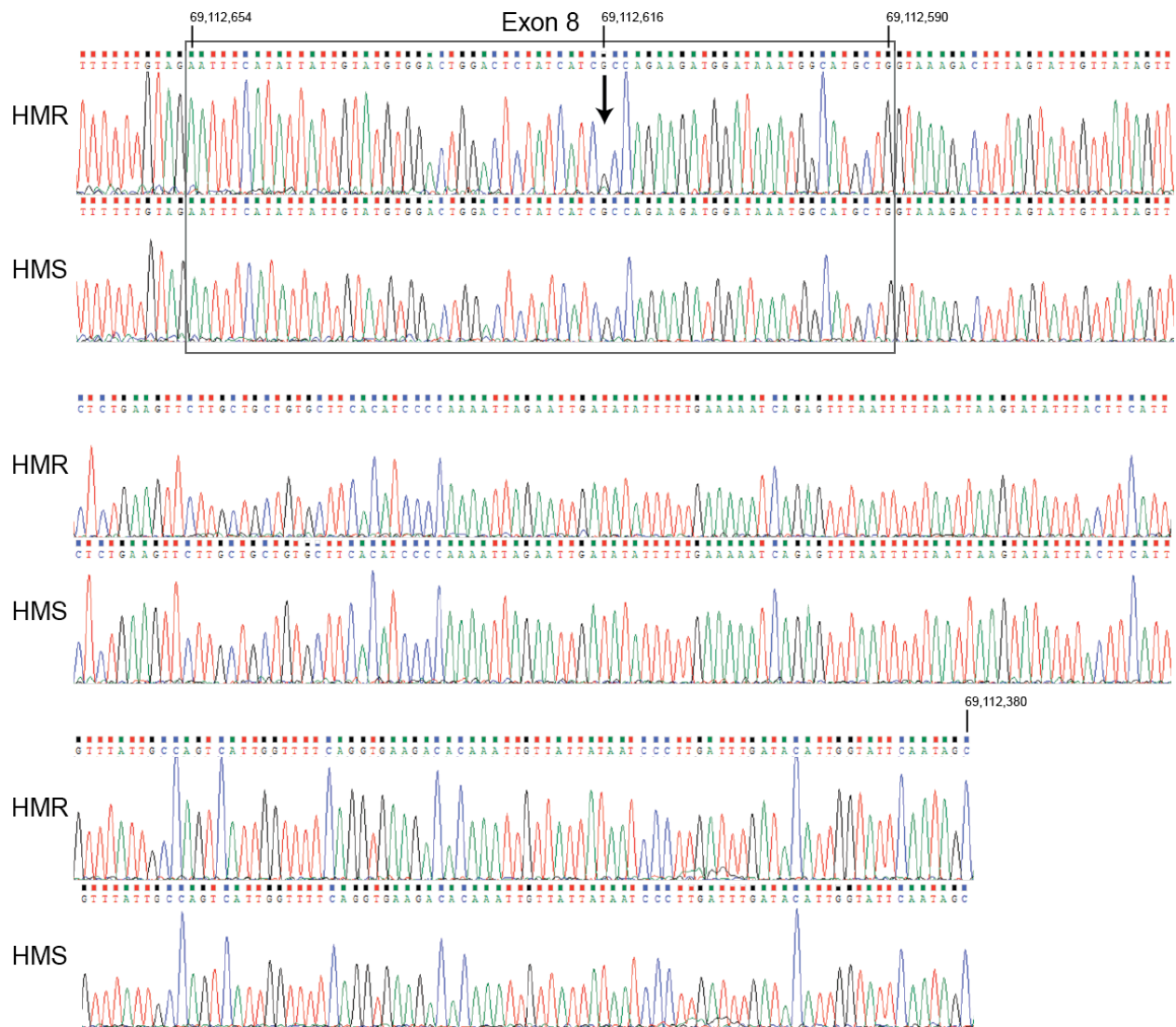
**Supplementary Figure 2 Expression of cytochrome P450 family genes.** RNA was generated from HMS (DMSO treated or treated with 3  $\mu$ M MLN494 for 8 or 24 hours) and HMR (grown constitutively in the presence of 3  $\mu$ M MLN4924) cells and transcripts were profiled using an Illumina Human HT-12 v4 Expression BeadChip microarray. After standardization, data sets were filtered for cytochrome P450 genes and clustered to evaluate changes in expression between the different cell lines and treatments. A heat map summarizing the experiment is shown with 3 replicates for each. Hierarchical clustering of standardized data did not identify any significant differences in expression of these genes in HMR cells relative to untreated HMS cells or HMS cells treated for 8 or 24 hours with 3  $\mu$ M MLN4924. From this study, we concluded that changes in the expression of these genes do not significantly contribute to decreased MLN4924 sensitivity found in HMR cells.



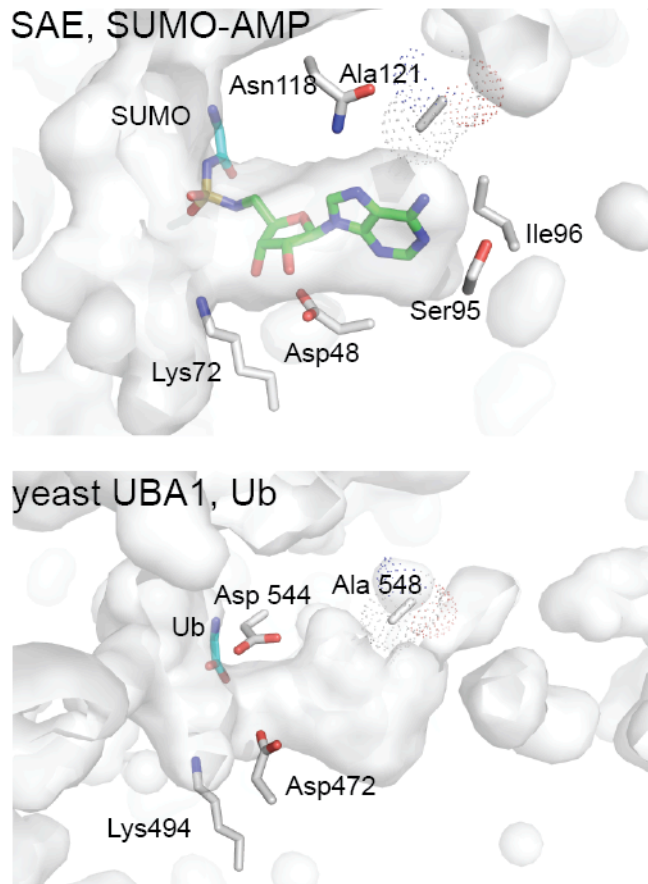
**Supplementary Figure 3 Ubiquitin conjugates in bortezomib and MLN4924 treated HMS and HMR cells.** Cell extracts from HMS and HMR cells treated with bortezomib (B) and MLN4924 (M) for the indicated times were analyzed by immunoblot for ubiquitin conjugates. GAPDH was used to verify normalized protein loading. High molecular weight ubiquitin conjugates are indicated.



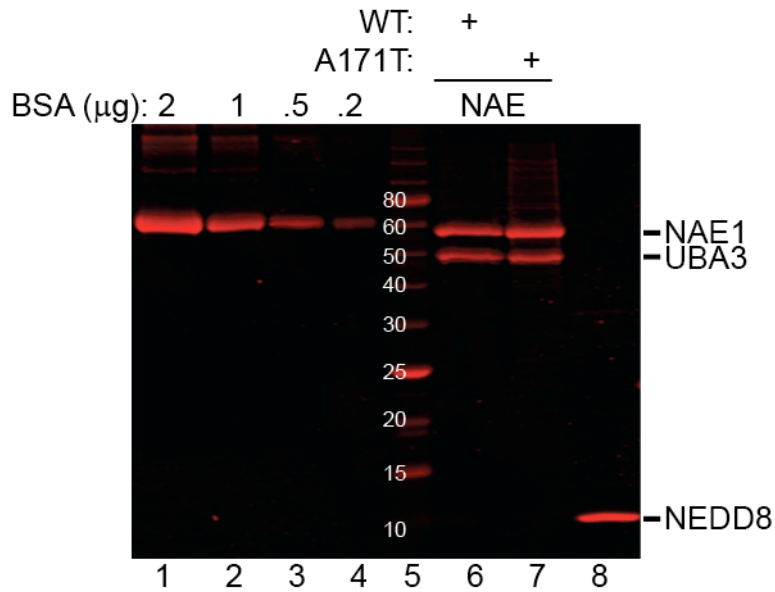
**Supplementary Figure 4 Sequences of UBA3 cDNAs cloned from HMR cells.** Chromatograms of UBA3 cDNAs cloned from HMS and HMR cells identify a single nucleotide transition found in HMR cDNAs. Sequences from nucleotide 463 to 561 are shown, with the identified G to A transition at 511 found in 3 out of 6 cDNAs from HMR cells indicated. All other sequences between HMS and HMR cDNAs were identical. The resulting amino acid sequences with the corresponding change in amino acid 171 from alanine to threonine found in HMR cells are shown. Numbering is based on UBA3 isoform 1.



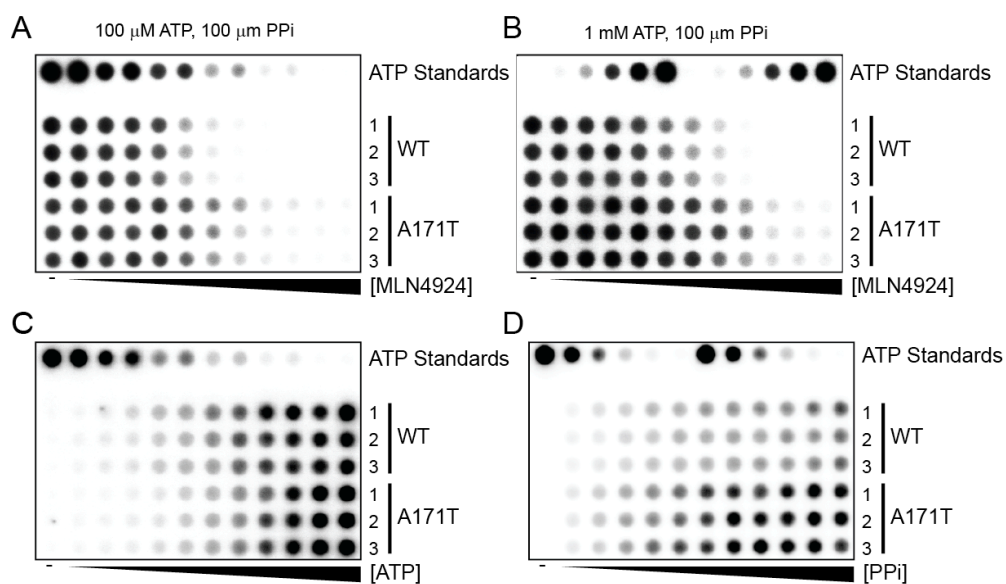
**Supplementary Figure 5 Extended genomic DNA sequence within the UBA3 nucleotide binding pocket around heterozygous sequences encoding A171 and A171T.** PCR amplified genomic DNAs corresponding to 69,112,979 to 69,112,115 of chromosome 3 from HMS and HMR cells were sequenced. The shown chromatograms (69,112,664 to 69,112,380) are an extended version of Fig. 2B and include exon 8 (boxed) and flanking intron sequences. The heterozygous purine transition (R, guanine and adenine) at 69,112,616 in HMR cells, but not HMS cells, is indicated.



**Supplementary Figure 6 Nucleotide binding pockets of SAE and yeast UBA1.** A similarly positioned alanine can be readily identified in the nucleotide binding pockets of the SUMO activating enzyme (SAE) and yeast ubiquitin-activating enzyme (UBA1). Alanine 121 of SAE in the SAE-SUMO-AMP ternary structure (PDB 3KYC) (Olsen et al., 2010) forms an edge of the solvent accessible nucleotide binding pocket that does not directly contact the adenine ring of AMP in the context of the SUMO-adenylate. Alanine 548 of yeast Uba1 has a similar position in the enzyme's nucleotide binding pocket. This model (PDB 3CMM) (Lee and Schindelin, 2008) contains a non-covalently bound ubiquitin molecule (Ub). Our observations for NAE and the presence of a similarly positioned alanine residue in these models and in alignments of all canonical E1s (see Fig. 2C) suggest the alanine participates in defining an edge of the nucleotide binding pocket. In these models, the solvent accessible pocket is shown as are side chains important in E1 activity.



**Supplementary Figure 7 Purified NAE, NAE (UBA3 A171T), and recombinant NEDD8.** The concentrations of purified NAE, NAE (UBA3 A171T), and NEDD8 were measured by coomassie staining of protein gels containing known amounts of BSA. Gels were scanned on a Licor Odyssey and analyzed using the instrument's software to quantify NAE and NEDD8 based on the resulting BSA standard curve . Protein molecular weight standards are indicated as well as NAE1, UBA3, and NEDD8.



**Supplementary Figure 8 Raw data from ATP:PPi exchange assays.** Phosphor screen scans show the NEDD8-dependent ATP generated by NAE and NAE (UBA3 A171T) in MLN4924 titrations using either 100  $\mu$ M (A) or 1 mM ATP (B). These experiments used 10 nM NAE or NAE (UBA3 A171T), 100  $\mu$ M (top panel) or 1 mM (bottom panel) ATP, 100  $\mu$ M PPi (with 50 cpm/pmol [ $^{32}$ P] PPi), and 1  $\mu$ M NEDD8. MLN4924 dilutions (11 2-fold serial dilutions in 0.025% final DMSO concentration or DMSO only) were added to reactions containing NAE, ATP, and PPi with NEDD8 added to start the reaction. Reactions were incubated for 30 minutes at 37°C prior to ATP purification on activated charcoal filter paper and filter processing. Known ATP concentrations (containing 50 cpm/pmol [ $\alpha$ - $^{32}$ P] ATP) in duplicate per filter (3-fold serial dilutions from 617 pmol to 2.54 pmol) were used to generate an ATP standard curve for quantification of NAE- and NEDD8-dependent ATP generation. (C) NEDD8-dependent NAE and NAE (UBA3 A171T) activity was measured in the presence of increasing concentrations of ATP in the ATP:PPi exchange assay. These experiments were performed as above, but using 1 mM PPi and 2-fold serial dilutions of ATP from 2 mM. (D) PPi titrations were performed to examine the NEDD8-dependent activities of NAE and NAE (UBA3 A171T) using 11 2-fold serial dilutions from 1 mM PPi and 10 nM NAE or NAE (UBA3 A171T), 2 mM ATP, and 1  $\mu$ M NEDD8.



## References

- Brownell, J. E., Sintchak, M. D., Gavin, J. M., Liao, H., Bruzzese, F. J., Bump, N. J., Soucy, T. A., Milhollen, M. A., Yang, X., Burkhardt, A. L., *et al.* (2010). Substrate-assisted inhibition of ubiquitin-like protein-activating enzymes: the NEDD8 E1 inhibitor MLN4924 forms a NEDD8-AMP mimetic in situ. *Mol Cell* 37, 102-111.
- Bruzzese, F. J., Tsu, C. A., Ma, J., Loke, H. K., Wu, D., Li, Z., Tayber, O., and Dick, L. R. (2009). Development of a charcoal paper adenosine triphosphate:pyrophosphate exchange assay: kinetic characterization of NEDD8 activating enzyme. *Anal Biochem* 394, 24-29.
- Lee, I., and Schindelin, H. (2008). Structural insights into E1-catalyzed ubiquitin activation and transfer to conjugating enzymes. *Cell* 134, 268-278.
- Olsen, S. K., Capili, A. D., Lu, X., Tan, D. S., and Lima, C. D. (2010). Active site remodelling accompanies thioester bond formation in the SUMO E1. *Nature* 463, 906-912.